

ESTIMATING EFFECT OF UNDULATOR FIELD ERRORS USING THE RADIATION HODOGRAPH METHOD

N.A. Sokolov[#], Budker INP, Novosibirsk, Russia
 N. Vinokurov, Russia, and KAERI, Daejeon, Rep. of Korea

Abstract

Spatially-periodic magnetic structures are widely used for generation of high-brilliance radiation in storage rings, sources of synchrotron radiation and free electron lasers. In 1947, V.L. Ginzburg suggested the first undulator scheme.

An alternating magnetic field created by a planar undulator makes electrons oscillate in the transverse direction, with interference of radiation emitted from separate parts of the trajectory. The spectrum of the forward emitted radiation is enhanced due to constructive interference.

The undulator is made of the magnetized bars that are not perfect and their magnetization differs. Therefore, the electron trajectory is not purely sinusoidal and, as a result, the spectral intensity fades. The task was to find out if the precision of magnet manufacturing is sufficient.

This paper presents modelling of electron motion in the measured magnetic field of the new (third) free electron laser at the Siberian Synchrotron Radiation Centre. We have managed to estimate the effect of the field errors through comparison of the resulting emitted field amplitude with the amplitude from ideal magnet bars using the hodograph method.

CALCULATING MAGNETIC FIELD OF UNDULATOR

The undulator under study consists of two rows of magnetized bricks with $1.5 \times 1.5 \text{ cm}^2$ square cross-section, a width w of 9 cm and alternating magnetization directions as shown in Fig. 1. A brick is characterized by homogeneous magnetization M and the brick shorter side b . The vertical component of the field of a brick, centered at the origin is given by two expressions for contributions of vertical M_y and horizontal M_z components of magnetizations. Now the undulator field can be calculated as the sum of the fields of all its bricks (Eq. 1):

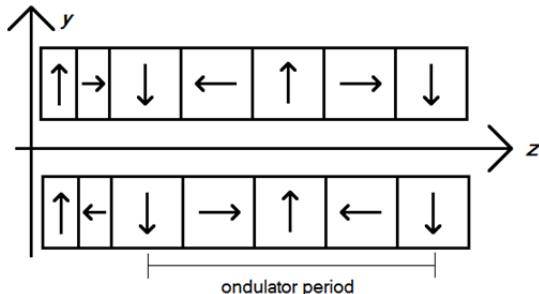


Figure 1: Scheme of permanent magnet undulator.

$$B_y(z) = 2 \sum_n \left[B_v(0, g, z - nb) \cos \frac{\pi n}{2} + B_h(0, g, z - nb) \sin \frac{\pi n}{2} \right], \quad (1)$$

where g is the distance between the undulator axis and the brick centres, and $M_y = M_z = M$. It should be taken into account that the undulator begins and ends with two pairs of halved bricks for the average angle of particle trajectory and the transverse coordinate to be the same at the undulator ends. The fields of these termination bricks were calculated with formula, similar to Eqs. 2 and 3. The contribution of termination bricks is skipped in Eq. 1, but was taken into account in field and trajectory calculations. Bricks with vertical (along the OY axis) magnetization change the particle transverse angle, while bricks magnetized horizontally along the OZ axis change the transverse coordinate of particle.

This results, for a magnetic field of ideal bricks, in an electron trajectory which is close to the undulator axis and has close-to-zero transverse angle and coordinate (see Fig. 2).

Since the average magnetization of brick M is not known precisely, let select it such that the ideal undulator field is close to the measured undulator field, shown in Fig. 3. We obtained an average magnetization of 1.076 kG using the method of standard deviations. The field errors, shown in Fig. 4, apparently do not exceed 5 % of the field maximum.

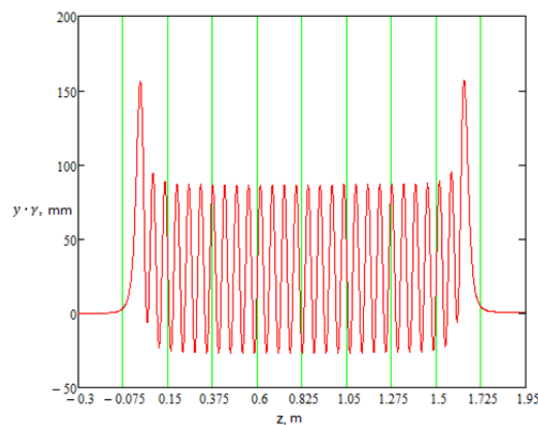


Figure 2: Electron trajectory in the field of the ideal undulator.

[#]faucct@gmail.com

$$B_y(x, y, z) = -M_y \operatorname{atan} \frac{(y-y')\sqrt{(x-x')^2 + (y-y')^2 + (z-z')^2}}{(x-x')(z-z')} \Bigg|_{x'=-w/2}^{x'=w/2} \Bigg|_{y'=-b/2}^{y'=b/2} \Bigg|_{z'=-b/2}^{z'=b/2}, \quad (2)$$

$$B_h(x, y, z) = M_z \ln \frac{\sqrt{(x-x')^2 + (y-y')^2 + (z-z')^2} - x + w/2}{\sqrt{(x-x')^2 + (y-y')^2 + (z-z')^2} - x - w/2} \Bigg|_{y'=-b/2}^{y'=b/2} \Bigg|_{z'=-b/2}^{z'=b/2}. \quad (3)$$

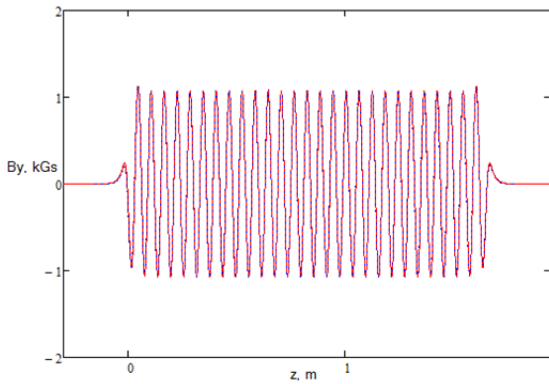


Figure 3: Measured undulator magnetic field.

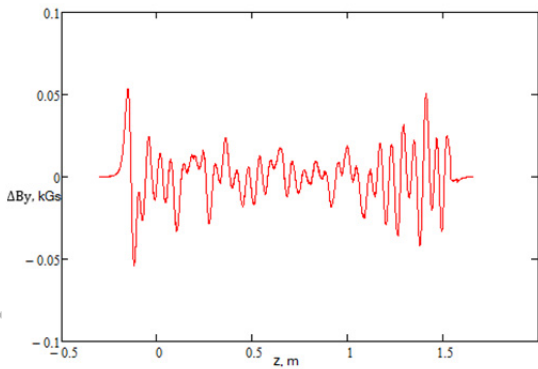


Figure 4: Difference in the fitted ideal and measured magnetic fields.

RADIATION HODOGRAPH METHOD

For a planar undulator the Fourier-harmonics of forward emitted radiation at frequency ω is proportional to [1]:

$$\int_{-\infty}^{\infty} e^{i\omega t(z) - i\omega z/c} \frac{dx}{dz}(z) dz, \quad (4)$$

where c is the velocity of light. Eq. 4 shows that it is sum of contributions of all segments of the particle trajectory. In a good undulator at some frequency phases of contributions of different segments are the same, and the modulus of the radiation Fourier-harmonics is maximum.

To visualize contributions of different parts of the undulator one can take the integral Eq. 4 from the undulator entrance to some current point z_1 . Calculating arrival time $t(z)$ and small deflection angle dx/dz through the measured field we define the hodograph function [2, 3] as

$$G(z_1) = \int_0^{z_1} I_{1y}(z) \exp\{-i\kappa[z + \int_0^z I_{1y}^2(z') dz']\} dz, \quad (5)$$

where the $I_{1y}(z)$ is the first integral of the magnetic field:

$$I_{1y}(z) = \frac{e}{mc^2} \int_0^z B_y(0,0,z') dz', \quad (6)$$

and $\kappa = \omega/(2\gamma^2 c)$. We can use this expression to estimate the magnetic field error if we draw the curve consisting of points with coordinates $\operatorname{Re}G(z_1)$, $\operatorname{Im}G(z_1)$.

CALCULATION OF MEASURED FIELD RADIATION HODOGRAPH

Let apply the hodograph formula Eq. 5 to the measured field of the undulator and then compare with the case of ideal field. We can calculate the particle trajectory with a 1 mm step in the z coordinate (see Fig. 5).

Let's calculate the hodograph applying the formula to these trajectories. The results are shown in Figs. 6 and 7.

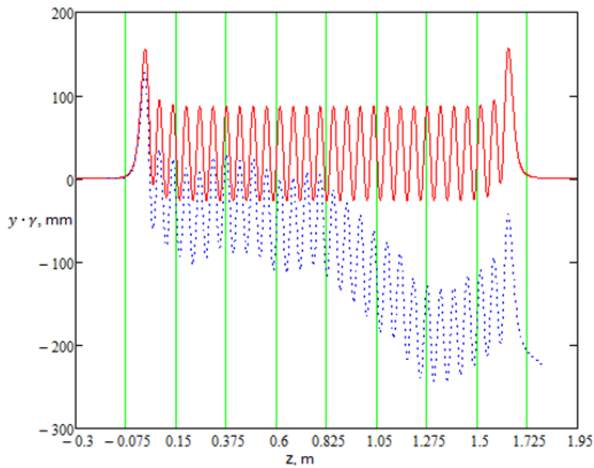


Figure 5: Particle transverse deviations multiplied by gamma. The red line represents trajectory in the ideal field; the blue line is for the measured field.

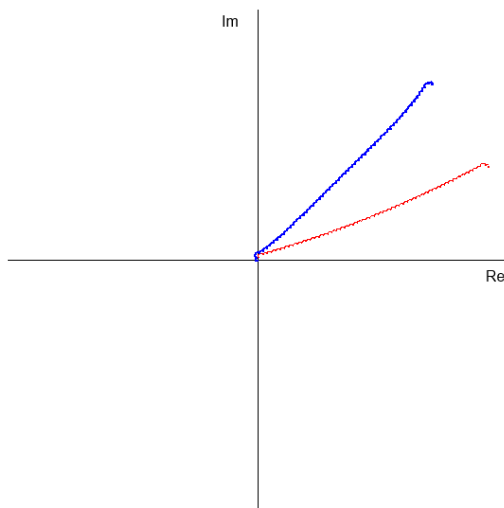


Figure 6: Measured and ideal field hodographs. Blue line: measured field, red line: ideal field.

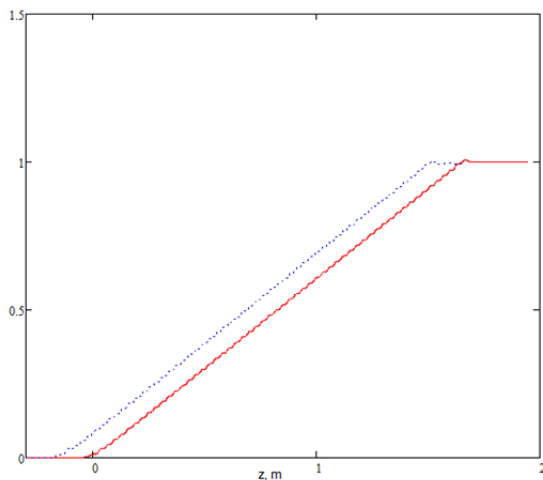


Figure 7: Hodographs' absolute value increments.

RESULTS

We can reach the emitted field amplitude maximums at $\kappa = 88.65m^{-1}$ and $88.61m^{-1}$ for ideal and measured fields accordingly. Maximum amplitude for a measured field is equal 0.995 of a maximum amplitude for an ideal field.

Building the emitted amplitude spectrum (Fig. 8), we can estimate the relative width of main peak equal 3.2%.

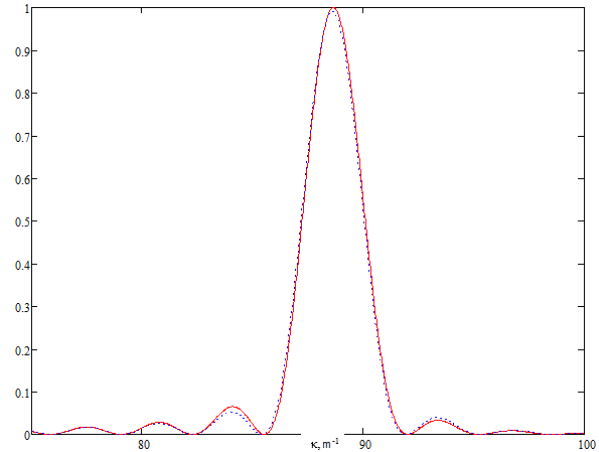


Figure 8: Radiation spectrum for measured (red) and ideal (blue) fields.

From comparing the amplitudes' maxima for the measured and ideal fields, it follows that we cannot enhance the spectral intensity in maximum more than by 1% neither by increasing the precision of magnet manufacturing, neither by increasing the precision of their spatial placement. That means that the measured field is good enough for generation of a monochromatic terahertz radiation.

ACKNOWLEDGMENT

This work is supported by Russian Science Foundation (project 14-12-00480).

REFERENCES

- [1] L.D. Landau and E.M. Lifshitz, *The Classical Theory of Fields*, Oxford, New York, Toronto, Sidney, Braunschweig: Pergamon Press, 1971, 172.
- [2] E. Gluskin et al., Nucl. Instr. And Meth. A475 (2001) 323.
- [3] E. Levichev and N. Vinokurov, Rev. Accel. Sci. Technol. **3** (2010) 203.